Molecular Cancer Research

Crystal Structure of a Multidomain Human p53 Tetramer Bound to the Natural *CDKN1A* (*p21*) p53-Response Element

Soheila Emamzadah[1], Laurence Tropia[1], and Thanos D. Halazonetis[1,2]

Abstract

The p53 tumor suppressor protein is a sequence-specific DNA-binding transcription factor. Structures of p53 bound to DNA have been described, but, so far, no structure has been determined of p53 bound to a natural p53-response element. We describe here the structure of a human p53 homotetramer encompassing both the DNA-binding and homo-oligomerization domains in complex with the natural p53-response element present upstream of the promoter of the *CDKN1A* (*p21*) gene. Similar to our previously described structures of human p53 tetramers bound to an artificial consensus DNA site, p53 DNA binding proceeds via an induced fit mechanism with loops L1 of two subunits adopting recessed conformations. Interestingly, the conformational change involving loop L1 is even more extreme than the one previously observed with the artificial consensus DNA site. In fact, the previously determined loop L1 conformation seems to be a transition intermediate between the non–DNA-bound and *CDKN1A*-bound states. Thus, the new structure further supports our model that recognition of specific DNA by p53 is associated with conformational changes within the DNA-binding domain of p53. *Mol Cancer Res; 9(11); 1493–9. ©2011 AACR.*

Introduction

The *p53* tumor suppressor gene regulates the response of cells to DNA damage (1, 2). It is the most frequently mutated gene in human cancer (3, 4), possibly to allow cancer cells to survive and proliferate in the presence of oncogene-induced DNA replication stress (5). The protein encoded by *p53* is a transcription factor containing 2 independently folding domains: a sequence-specific DNA-binding domain at the center of the protein and a homotetramerization domain toward its C-terminus (6–8).

Three-dimensional structures of p53 have been determined both in its free and DNA-bound forms (9–15). From the protein side, these structures encompass either only the sequence-specific DNA-binding domain (9–14) or a larger polypeptide that includes both the DNA-binding and homo-oligomerization domains (15). The first group of structures shows no conformational change in the p53 DNA-binding domain upon interaction with DNA, which is atypical of sequence-specific DNA-binding proteins (16–18). In contrast, the structures of the multidomain p53 tetramer bound to DNA show a conformational switch involving loops L1 of the DNA-binding domains of 2 p53 subunits (15). We have argued that this conformational switch allows p53–DNA binding on-rates and off-rates to be regulated independently of dissociation rates. Thus, complexes of p53 with specific DNA have much longer half-lives than complexes with nonspecific DNA, even though the affinities of p53 for specific and nonspecific DNA differ by less than 10-fold (15, 19). Such a model to explain DNA-binding specificity could be generally applicable, as conformational switching is a feature of all characterized sequence-specific protein–DNA interactions (20).

Despite the great progress made towards structural characterization of p53–DNA complexes, none of the structures determined so far contain a natural p53-response element. To address this gap, we crystallized a multidomain p53 polypeptide bound to the well-characterized p53-response element present upstream of the promoter of the *CDKN1A* (also known as *p21*, *WAF1*, and *CIP1*) gene (21–26).

Materials and Methods

Protein sample preparation and crystallization

The p53 polypeptide p53CR2 (15) was expressed in *E. coli*. The cells were lysed in buffer consisting of 25 mmol/L Bis-Tris propane (pH 6.8), 250 mmol/L NaCl, 5 mmol/L dithiothreitol, and protease inhibitors, and the polypeptides were purified by cation exchange (Sepharose SP column; Pharmacia Biotech) and gel filtration (Superdex 200 column; Pharmacia Biotech) chromatography. After purification, the p53 protein was incubated

Authors' Affiliations: Departments of [1]Molecular Biology and [2]Biochemistry, University of Geneva, Geneva, Switzerland

Corresponding Author: Thanos D. Halazonetis, Department of Molecular Biology, University of Geneva, 30, quai Ernest-Ansermet, Geneva CH-1205, Switzerland. Phone: 41-22-379-6112; Fax: 41-22-379-6868; E-mail: thanos.halazonetis@unige.ch

doi: 10.1158/1541-7786.MCR-11-0351

with DNA at a 1:1.1 protein:DNA molar ratio at 4°C for 1 hour in 25 mmol/L Bis-Tris propane (pH 6.8), 150 mmol/L NaCl, and 5 mmol/L dithiothreitol buffer. The complex was then purified by gel filtration chromatography (Superdex 200 column; Pharmacia Biotech), concentrated to about 8 mg/mL protein concentration and crystallized at 4°C under standard hanging drop vapor diffusion conditions in 48-well plates (Hampton Research). The precipitant solution used for crystallization consisted of 0.2 mol/L potassium sodium tartrate tetrahydrate (pH 7.0) and 20% polyethylene glycol 3350. The sequence of the DNA used for crystallization is shown in Fig. 1A.

Data collection and structure refinement

X-ray diffraction data sets were collected at the ID23-2 microfocus beamline of the European Synchrotron Radiation Facility. Reflection data were indexed, integrated, and scaled with the CCP4 software package (27). Initial solutions were determined by molecular replacement and refined under noncrystallographic symmetry restraints for the protein chains with the programs CNS and O (28, 29). Figures were prepared with the programs MOLSCRIPT, BOBSCRIPT, and RASTER3D (30–32).

Results

Overall structure

The p53 protein used in this study has been previously characterized and described as protein p53CR2 (15). It spans residues 94 to 358 of human p53 and encompasses the sequence-specific DNA-binding (residues: 94–291) and homo-oligomerization (residues: 324–355) domains, but contains a deletion of residues 293 to 321, which correspond to the flexible linker between these domains. The sequence-specific DNA-binding domain in p53CR2 has been engineered to prevent aggregation and unfolding *in vitro*. This was accomplished by introducing 13 amino acid substitutions targeting nonconserved residues that are far away from the DNA-binding surface. The goal of these substitutions was to enhance the contribution of the hydrophobic effect to protein folding. Analysis of the stabilized p53 DNA-binding protein both *in vitro* and in cell-based assays showed that the engineered amino acid substitutions had no effect on DNA-binding specificity and tumor suppressor function (15). In addition to the amino acid substitutions in the DNA-binding domain, the p53CR2 protein contains in its oligomerization domain 2 amino acid substitutions that only allow homodimer formation. However, when incubated

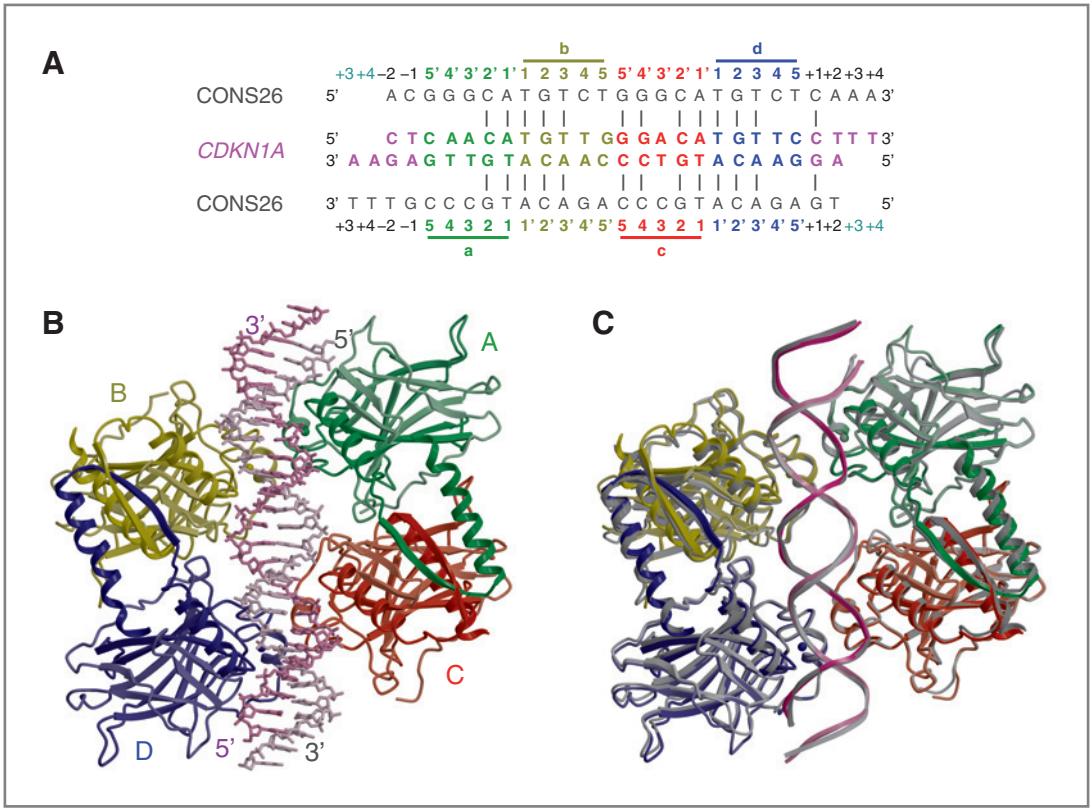

Figure 1. Overall 3-dimensional structure of a multidomain p53 oligomer bound to the *CDKN1A*–p53-response element. A, sequence of the oligonucleotides containing the *CDKN1A*–p53-response element (*CDKN1A*), and comparison to the sequence of oligonucleotides (CONS26) containing an artificial consensus p53-binding site. The p53-binding site consists of 4 contiguous pentamer repeats (a–d). B, overall 3-dimensional structure of 2 p53CR2 dimers bound to the *CDKN1A*–p53-response element. The p53 subunits are labeled A–D, corresponding to the DNA pentamer repeats a–d, respectively. C, superimposition of the p53CR2–*CDKN1A* (colored) and p53CR2–CONS26 (gray; ref. 15) structures.

with sequence-specific DNA sites, 2 p53CR2 dimers form a stable complex with DNA, thereby recapitulating the binding of p53 homotetramers to DNA (15).

The oligonucleotides used for crystallization anneal to form DNA that is 24 bp long with overhangs that are 2 nucleotides long at each 3′ end (Fig. 1A). The overhangs were designed to allow formation of pseudocontinuous DNA molecules through the crystal, as was, indeed, the case. The 24-bp sequence corresponds to the natural p53-response element present in the human *CDKN1A* (*p21*) gene (20 bp) plus the natural flanking sequences (2 bp on each side). The p53-response element consists of 4 contiguous pentamer repeats, which we have labeled a, b, c, and d, reflecting their 5′ to 3′ order in the DNA sequence (Fig. 1A). Repeats b and c, which are at the center of the p53–DNA-binding site, are referred to as the inner repeats, whereas repeats a and d are the outer repeats. Of note, the *CDKN1A*–p53-response element has only 60% identity to the artificial consensus site (oligonucleotide CONS26) that we previously crystallized bound to p53CR2 (Fig. 1A; ref. 15).

The 3-dimensional structure of 2 p53CR2 dimers bound to the *CDKN1A*–p53-response element was determined at a resolution of 2.8 Å (Fig. 1B and Table 1). The overall structure is very similar to the previously determined structure of p53CR2 bound to oligonucleotide CONS26 (Fig. 1C). Thus, the *CDKN1A*–p53-response element exhibits the same helical axis shift at its center, as previously described for CONS26, and all the base pairing is of the Watson–Crick type. The intersubunit contacts between the 4 p53–DNA-binding domains are also identical to those previously described for the p53CR2–CONS26 DNA complex (15). Nevertheless, despite the high level of overall similarity between the p53CR2–*CDKN1A* and p53CR2–CONS26 structures, there are also interesting differences, as will be described later. We will be referring to the p53 subunits as A, B, C, and D, matching the label of the pentamer repeat, whose major groove they contact (Fig. 1A and B).

p53 DNA contacts

As in the previously described p53CR2–CONS26 DNA structure, there are similarities and differences in the way the p53 subunits recognize the inner and outer repeats. The sequence-specific contacts involve predominantly bp 2 and 3 of each pentamer repeat and are similar for all p53 subunits. Using subunit B as an example, one observes the previously described hydrogen bonds between Arg280 and the O6 and N7 atoms of the guanine base at position 2 of repeat b (Fig. 2A and B). The sugar backbone of the same nucleotide and the sugar backbone of the thymidine at position 3 are in contact with the side chain of Arg248 of subunit A (Fig. 2B). From the side of the major groove, the thymine at position 3 of repeat b forms a hydrogen bond with the side chain of Cys277 of subunit B (Fig. 2A and C). In addition, van der Waals and hydrophobic interactions stabilize the C5A atom of the thymine at an equidistant position between the side chains of Ala276 and Cys277. In the *CDKN1A*–p53-response element, a thymine is present at position 3 in all 4 pentamer repeats (Fig. 1A), perhaps helping in explaining the high affinity of the *CDKN1A* element for p53.

Unlike the contacts of p53 with bp 2 and 3, which are essentially identical in all 4 subunits, the interactions with bp 4 and 5 vary depending on whether the p53 subunit contacts an inner or an outer repeat. This is because the conformation of loop L1 is different in the inner and outer p53 subunits. In the inner subunits, loop L1 adopts an extended conformation, the same conformation that is also observed in the absence of DNA. This extended conformation is accommodated thanks to the shift in the DNA helical axis, which

Table 1. Data collection and refinement statistics for the p53CR2–*CDKN1A* structure

Data collection	
X-ray wavelength	0.87260 Å
Space group	*P*21212
Cell dimensions, Å	*a* = 163.81
	b = 169.20
	c = 55.26
Resolution, Å	52.34–2.80 (2.95–2.80)
Observations	187,355 (27,369)
Unique reflections	35,732 (5,267)
Data coverage, %	93.3 (95.0)
$\langle I/\sigma(I)\rangle$	12.4 (3.0)
*R*sym,[a] %	12.0 (41.6)
Refinement statistics	
Resolution range, Å	50.0–2.80
Reflections used, >0 sig*F*	35,703
Protein atoms	7,452
Zn atoms	4
DNA atoms	1,060
Water molecules	105
R factor,[b] %	23.6
Rfree,[c] %	28.3
RMS deviations[d]	
Bonds, Å	0.006
Angles, degree	1.01
Ramachandran plot	
Most favored, %	79.0
Allowed, %	20.3
Generously allowed, %	0.7
Disallowed, %	0.0

NOTE: Values in parentheses refer to the highest resolution shell.

[a] $R_{sym} = \Sigma_h \Sigma_i |I_{h,i} - I_h| / \Sigma_h \Sigma_i I_{h,i}$ for the intensity (I) of *i* observations of reflection *h*.

[b] R factor $= \Sigma |F_{obs} - F_{calc}| / \Sigma |F_{obs}|$, where F_{obs} and F_{calc} are the observed and calculated structure factors, respectively.

[c] R_{free} = R factor calculated with 5% of the reflection data chosen randomly and omitted from the start of refinement.

[d] RMS deviations for bonds and angles are the respective root mean square deviations from ideal values.

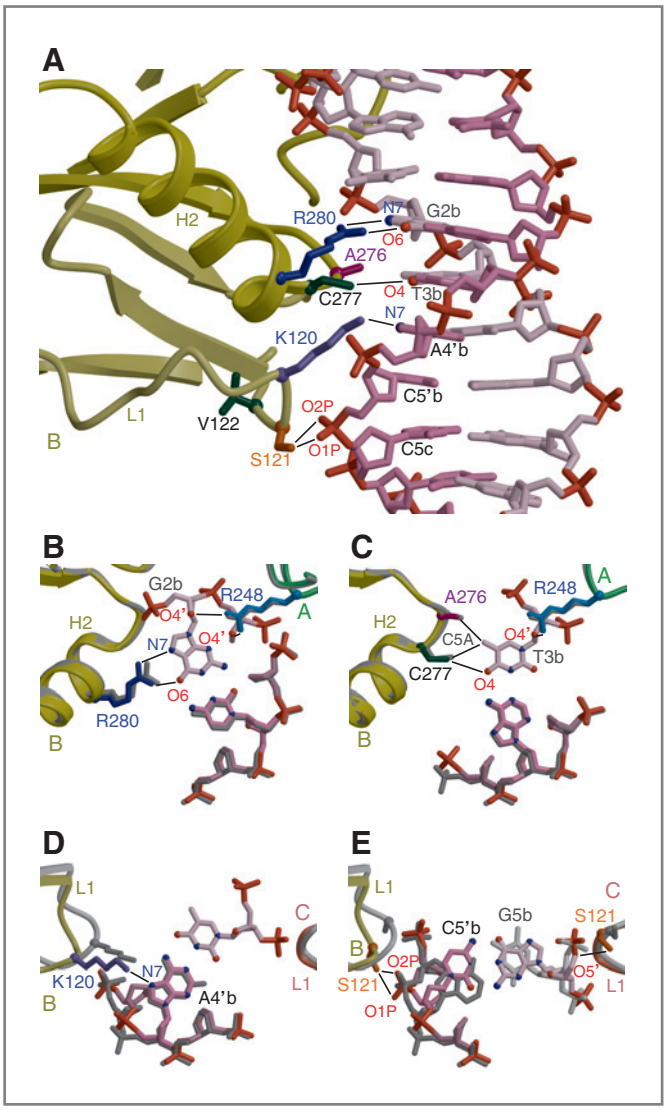

Figure 2. p53CR2–*CDKN1A* contacts involving an inner pentamer repeat (repeat b). A, interactions of residues Arg280 (R280), Ala276 (A276), Cys277 (C277), Lys120 (K120), and Ser121 (S121) of subunit B with DNA. In this and all subsequent panels, the main chains are colored as in Fig. 1B. H2, helix 2 of the DNA-binding domain; L1, loop L1. B, interactions of Arg280 of subunit B (R280) and Arg248 of subunit A (R248) with the guanosine nucleotide at position 2 of repeat b (G2b). In this and all subsequent panels, the corresponding elements of the p53CR2–CONS26 structure are also shown (gray). For clarity, not all DNA atoms are shown. C, interactions of Ala276 (A276) and Cys277 (C277) of subunit B with the thymine base at position 3 of repeat b (T3b). D, interaction of Lys120 (K120) of subunit B with the adenine base at position 4′ of repeat b (A4′b). E, interactions of Ser121 (S121) of subunit B with the cytidine at position 5′ of repeat b (C5′b).

moves the DNA backbone away from loop L1, relative to B-form DNA. In contrast, in the outer subunits, loop L1 adopts a recessed conformation to avoid steric clashes with the DNA, which here adopts the standard B-form DNA (15).

Using p53 subunit B as an example of the contacts of subunits B and C to the inner repeats b and c, respectively, the side chain of Lys120 makes a hydrogen bond with atom N7 of the adenine base at position 4′ of repeat b (Fig. 2A and D). Furthermore, the side chain of Ser121 makes hydrogen bonds with the sugar–phosphate backbone of the cytidine at position 5′ of repeat b (Fig. 2A and E).

In p53 subunit A, representing the contacts of subunits A and D to the outer repeats a and d, respectively, Lys120 does not contact DNA, whereas, the side chain of Ser121 contacts the phosphate backbone of the nucleotide 3 positions 5′ to the p53-response element (Fig. 3A). In addition, Arg283 contacts the phosphate backbone of the cytidine at position 5′ of repeat a (Fig. 3A). The corresponding cytidine in repeat b is contacted by the side chain of Ser121 of subunit B (compare with Fig. 2A).

Table 2 summarizes all the p53–DNA contacts observed in the p53CR2–*CDKN1A* structure.

Loop L1 conformations

The structure of p53CR2 bound to the *CDKN1A*–p53-response element shows 2 distinct loop L1 conformations; an extended conformation for the inner subunits (Fig. 2A) and a recessed conformation for the outer subunits (Fig. 3A). The p53CR2–CONS26 structure also displayed extended and recessed conformations (15). The extended loop L1 conformations of the p53CR2–*CDKN1A* and p53CR2–CONS26 structures are very similar to each other and to the conformation of loop L1 in free p53 (15 and data not shown). However, the recessed conformations in the p53CR2–*CDKN1A* and p53–CONS26 structures differ. In p53CR2–*CDKN1A*, the side chain of Val122 faces towards the protein interior, as expected for a hydrophobic residue, whereas the side chain of

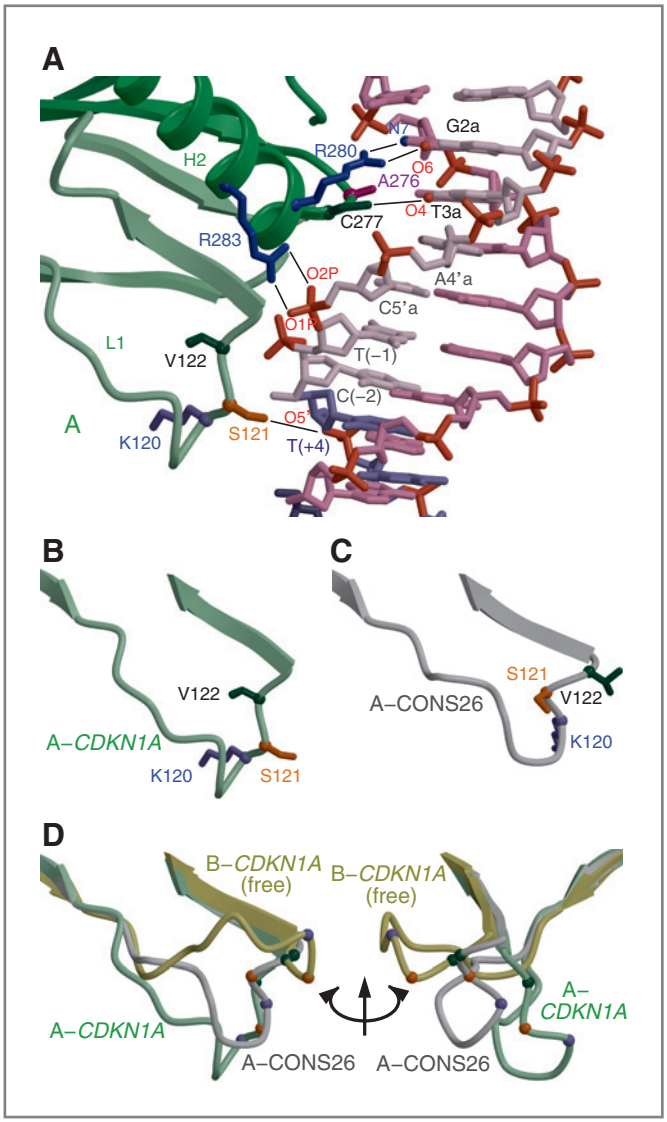

Figure 3. p53CR2–*CDKN1A* contacts involving an outer pentamer repeat (repeat a) and comparison of loop L1 conformations. A, interactions of residues Arg280 (R280), Ala276 (A276), Cys277 (C277), Arg283 (R283), and Ser121 (S121) of subunit A with DNA. In this and all subsequent panels, the main chains are colored as in Fig. 1B. The crystallographic symmetry-related DNA next to subunit A is colored blue. H2, helix 2 of the DNA-binding domain; L1, loop L1. B, conformation of loop L1 of subunit A of p53CR2 bound to the *CDKN1A*–p53-response element. The side chains of Lys120 (K120), Ser121 (S121), and Val122 (V122) are shown. The orientation is the same as in A. C, conformation of loop L1 of subunit A of p53CR2 bound to a consensus DNA site (CONS26; ref. 15). The side chains of Lys120 (K120), Ser121 (S121), and Val122 (V122) are shown. The orientation is the same as in A. D, superimposition of loops L1 of subunits A and B of the p53CR2–*CDKN1A* structure and loop L1 of subunit A of the p53CR2–CONS26 structure. The orientation on the left side is the same as in A–C. On the right side, the structures have been rotated by 80 degrees and are viewed from the side of the DNA. The α-carbon atoms of Lys120, Ser121, and Val122 are colored blue, orange, and dark green, respectively. The conformation of loop L1 of p53 in the non–DNA-bound (free) state is essentially the same as that of subunit B in the DNA-bound state.

Ser121 faces away from the protein interior and contacts the DNA backbone (Fig. 3A and B). In contrast, in p53CR2–CONS26, the side chain of Val122 faces towards solvent, whereas the side chain of Ser121 faces somewhat towards the protein interior and fails to contact DNA (Fig. 3C and ref. 15).

Superimposition of the 3 loop L1 conformations (extended, recessed CONS26, and recessed *CDKN1A*) reveals that the recessed CONS26 conformation is intermediate between the extended and recessed *CDKN1A* conformations (Fig. 3D). Specifically, the conformational switch between the extended and recessed CONS26 conformations does not affect the position of the α-carbon atom of Val122; whereas, in the recessed *CDKN1A* conformation the α-carbon atom of Val122 has moved 6.5 Å away (Fig. 3D). It is important to note that in both the p53CR2–CONS26 and p53CR2–*CDKN1A* structures, loops L1 do not participate in crystal packing contacts and, therefore, their conformation cannot be a crystal packing artifact.

Discussion

We report here the first, to our knowledge, 3-dimensional structure of p53 bound to a natural response element. The structure recapitulates well the features observed previously in the complex of a multidomain p53 tetramer bound to a consensus DNA site. Thus, it provides additional support for our conclusion that binding of p53 to specific DNA sites is accompanied by conformational changes in the p53–DNA-binding domain, which, in turn, regulate the half-life of the p53–DNA complex (15).

Perhaps the most interesting feature of the p53CR2–*CDKN1A* structure is the novel conformation of loop L1 of the outer subunits. This novel conformation is satisfying in the sense that the hydrophobic side chain of Val122 points towards the protein interior and the side chain of Ser121 contacts the DNA phosphate backbone (Fig. 3A). In the extended loop L1 conformation, the side chain of Val122

Table 2. Protein–DNA contacts observed in the p53CR2–*CDKN1A* structure

Residue	Subunit A Nucleotide:atom	Subunit B Nucleotide:atom	Subunit C Nucleotide:atom	Subunit D Nucleotide:atom
K120	—	A4′b:N7	G4′c:N7	—
S121	symT(+4):O5′	C5′b:O1P C5′b:O2P	G5b:O5′	A(+2):O1P
N239	—	G2b:O1P	G2c:O1P	—
S241	G2a:O1P	G2b:O1P T1b:O3′	G2c:O1P T1c: O3′	G2d:O1P T1d:O3′
R248	G2b:O4′ T3b:O4′	T3a:O4′ T1b:O4′	T4d:O1P T3d:O3′	G2c:O4′
R273	T1a:O2P T1a:O5′	T1b:O2P T1b:O5′	T1c:O2P T1c:O5′	T1d:O2P T1d:O5′
A276	T3a:C5A	T3b:C5A	T3c:C5A	T3d:C5A
A276 (N)	G2a:O2P	G2b:O2P	G2c:O2P	G2d:O2P
C277	T3a:O4	T3b:O4	T3c:O4	T3d:O4
R280	G2a:N7 G2a:O6	G2b:N7 G2b:O6	G2c:N7 G2c:O6	G2d:N7 G2d:O6
R283	C5′a:O1P C5′a:O2P	—	—	G5′d:O2P

NOTE: The nucleotides and p53 subunits are defined as described in Fig. 1.
Abbreviations: sym, nucleotide from a symmetry-related molecule; (*N*), backbone amide group.

also faces towards the protein interior and Ser121 contacts the DNA (Fig. 2A). However, the α-carbon atoms of Val122 and Ser121 have moved 6.5 and 10.4 Å, respectively, between the extended and p53CR2–*CDKN1A* recessed conformations (Fig. 3D).

The recessed loop L1 conformation in the previously determined p53CR2–CONS26 structure can be seen to adopt a conformation that is intermediate between the extended and recessed p53CR2–*CDKN1A* conformations (Fig. 3D). One could argue that loop L1 adopts many different conformations according to the DNA sequence being contacted. Formally, we cannot exclude this possibility. In fact, different loop L1 conformations may allow p53 to exhibit different DNA-binding kinetics for different DNA sites, which would translate in different half-lives of the p53–DNA complexes (15). However, it is also possible that the p53CR2–CONS26 structure has trapped a transition intermediate between the extended and recessed p53CR2–*CDKN1A* conformations. This latter possibility is attractive because the solvent-exposed hydrophobic side chain of Val122 observed in the p53CR2–CONS26-recessed conformation (Fig. 3C) could serve to enhance the kinetic barrier for the conformational switch. Once, this barrier is bypassed, the side chain of Val122 would again face towards the protein interior (Fig. 3B), stabilizing the DNA-bound recessed p53–*CDKN1A* conformation. In support of this possibility, we have already shown that substitutions of Val122 with Gly or Ser decrease the half-life of sequence-specific p53–DNA complexes without an accompanying decrease in affinity (15). Determination of structures of p53 bound to a variety of natural and consensus p53-response elements will help elucidate the spectrum of loop L1 conformations and their role in regulating the DNA-binding properties of p53.

Disclosure of Potential Conflicts of Interest

No potential conflicts of interest were disclosed.

Acknowledgments

The authors thank the staff of the ESRF, Grenoble, France for help in collecting the X-ray diffraction data. Three-dimensional structure coordinates and structure factors have been deposited at the Protein Data Bank under the accession number 3TS8.

Grant Support

This work was supported by a Swiss National Foundation grant to T. D. Halazonetis.

The costs of publication of this article were defrayed in part by the payment of page charges. This article must therefore be hereby marked *advertisement* in accordance with 18 U.S.C. Section 1734 solely to indicate this fact.

Received July 25, 2011; revised September 14, 2011; accepted September 16, 2011; published OnlineFirst September 20, 2011.

References

1. Kastan MB, Onyekwere O, Sidransky D, Vogelstein B, Craig RW. Participation of p53 protein in the cellular response to DNA damage. Cancer Res 1991;51:6304–11.
2. Kuerbitz SJ, Plunkett BS, Walsh WV, Kastan MB. Wild-type p53 is a cell cycle checkpoint determinant following irradiation. Proc Natl Acad Sci U S A 1992;89:7491–5.

3. Hollstein M, Sidransky D, Vogelstein B, Harris CC. p53 mutations in human cancers. Science 1991;253:49–53.
4. Kan Z, Jaiswal BS, Stinson J, Janakiraman V, Bhatt D, Stern HM, et al. Diverse somatic mutation patterns and pathway alterations in human cancers. Nature 2010;466:869–73.
5. Halazonetis TD, Gorgoulis VG, Bartek J. An oncogene-induced DNA damage model for cancer development. Science 2008;319:1352–5.
6. Farmer G, Bargonetti J, Zhu H, Friedman P, Prywes R, Prives C. Wild-type p53 activates transcription *in vitro*. Nature 1992;358:83–6.
7. Vogelstein B, Lane D, Levine AJ. Surfing the p53 network. Nature 2000;408:307–10.
8. Vousden KH, Prives C. Blinded by the light: the growing complexity of p53. Cell 2009;137:413–31.
9. Cho Y, Gorina S, Jeffrey PD, Pavletich NP. Crystal structure of a p53 tumor suppressor-DNA complex: understanding tumorigenic mutations. Science 1994;265:346–55.
10. Kitayner M, Rozenberg H, Kessler N, Rabinovich D, Shaulov L, Haran TE, et al. Structural basis of DNA recognition by p53 tetramers. Mol Cell 2006;22:741–53.
11. Kitayner M, Rozenberg H, Rohs R, Suad O, Rabinovich D, Honig B, et al. Diversity in DNA recognition by p53 revealed by crystal structures with Hoogsteen base pairs. Nat Struct Mol Biol 2010;17:423–9.
12. Ho WC, Fitzgerald MX, Marmorstein R. Structure of the p53 core domain dimer bound to DNA. J Biol Chem 2006;281:20494–502.
13. Malecka KA, Ho WC, Marmorstein R. Crystal structure of a p53 core tetramer bound to DNA. Oncogene 2009;28:325–33.
14. Chen Y, Dey R, Chen L. Crystal structure of the p53 core domain bound to a full consensus site as a self-assembled tetramer. Structure 2010;18:246–56.
15. Petty TJ, Emamzadah S, Costantino L, Petkova I, Stavridi ES, Saven JG, et al. An induced fit mechanism regulates p53 DNA binding kinetics to confer sequence specificity. EMBO J 2011;30:2167–76.
16. Frankel AD, Kim PS. Modular structure of transcription factors: implications for gene regulation. Cell 1991;65:717–9.
17. Alber T. Protein-DNA interactions: how GCN4 binds DNA. Curr Biol 1993;3:182–4.
18. Spolar RS, Record MT Jr. Coupling of local folding to site-specific binding of proteins to DNA. Science 1994;263:777–84.
19. Weinberg RL, Veprintsev DB, Fersht AR. Cooperative binding of tetrameric p53 to DNA. J Mol Biol 2004;341:1145–59.
20. Tubbs JL, Tainer JA. p53 conformational switching for selectivity may reveal a general solution for specific DNA binding. EMBO J 2011;30:2099–100.
21. El-Deiry WS, Tokino T, Velculescu VE, Levy DB, Parsons R, Trent JM, et al. WAF1, a potential mediator of p53 tumor suppression. Cell 1993;75:817–25.
22. Xiong Y, Hannon GJ, Zhang H, Casso D, Kobayashi R, Beach D. p21 is a universal inhibitor of cyclin kinases. Nature 1993;366:701–4.
23. Harper JW, Adami GR, Wei N, Keyomarsi K, Elledge SJ. The p21 Cdk-interacting protein Cip1 is a potent inhibitor of G1 cyclin-dependent kinases. Cell 1993;75:805–16.
24. Szak ST, Mays D, Pietenpol JA. Kinetics of p53 binding to promoter sites *in vivo*. Mol Cell Biol 2001;21:3375–86.
25. Barlev NA, Liu L, Chehab NH, Mansfield K, Harris KG, Halazonetis TD, et al. Acetylation of p53 activates transcription through recruitment of coactivators/histone acetyltransferases. Mol Cell 2001;8:1243–54.
26. Kaeser MD, Iggo RD. Chromatin immunoprecipitation analysis fails to support the latency model for regulation of p53 DNA binding activity *in vivo*. Proc Natl Acad Sci U S A 2002;99:95–100.
27. CCP4 (Collaborative Computational Project, Number 4). The CCP4 suite: programs for protein crystallography. Acta Crystallogr D Biol Crystallogr 1994;50:760–3.
28. Brunger AT, Adams PD, Clore GM, DeLano WL, Gros P, Grosse-Kunstleve RW, et al. Crystallography and NMR system: a new software suite for macromolecular structure determination. Acta Crystallogr D Biol Crystallogr 1998;54:905–21.
29. Jones TA, Zou JY, Cowan SW, Kjeldgaard M. Improved methods for building protein models in electron density maps and the location of errors in these models. Acta Crystallogr A 1991;47:110–9.
30. Kraulis P. Molscript: a program to produce both detailed and schematic plots of protein structures. J Appl Crystallogr 1991;24:946–50.
31. Esnouf RM. An extensively modified version of Molscript that includes greatly enhanced coloring capabilities. J Mol Graph Model 1997;15:132–4.
32. Merritt EA, Bacon DJ. Raster3D: photorealistic molecular graphics. Methods Enzymol 1997;277:505–24.